Finding a Single Equation to Represent Urea Evaporation, Sublimation, and Decomposition in Selective Catalytic Reduction Systems

Noah Hertzler

A Senior Thesis submitted in partial fulfillment
of the requirements for graduation
in the Honors Program
Liberty University
Spring 2020

Acceptance of Senior Honors Thesis

This Senior Honors Thesis is accepted in partial
fulfillment of the requirements for graduation from the
Honors Program of Liberty University.

_____
Tom Eldredge, Ph.D.
Thesis Chair

_____
Hector Medina, Ph.D.
Committee Member

_____
David Schweitzer, Ph.D.
Assistant Honors Director

_____
Date

Abstract

Aqueous Urea used in Selective Catalytic Reduction (SCR) Systems undergoes three sequential processes that result in ammonia being produced to reduce harmful NOx emissions: Water evaporation, Urea sublimation, and Urea decomposition into ammonia and isocyanic acid. While these phases can be simplified by modeling the Urea as pure water, accuracy is sacrificed to do so. In order to make SCR modelling both accurate and simple, this project set out to find an equation that could represent all three processes. Simulations were run in ANSYS and Particle to generate a set of data, then an empirical equation was created to model these results. The final equation accurately models the evaporation and sublimation phases of Urea in SCR Systems. The decomposition process was not incorporated into the equation but will be the subject of future work.

Finding a Single Equation to Represent Urea Evaporation, Sublimation, and Decomposition in Selective Catalytic Reduction Systems

Introduction

Introduction to SCR Systems

While modern technology has greatly improved the average person's life over the years, the buildup of harmful pollutants in the atmosphere that results from vehicles and power plants has become a significant concern. One such group of pollutants is Nitrous Oxides (NOx), a term that classifies molecules made up of Nitrogen and Oxygen (NO, NO_2, etc.). These gasses are responsible for environmental concerns such as smog and acid rain ("What is Acid Rain?", n.d.).

One technology for reducing the release of these chemicals from combustion sources is Selective Catalytic Reduction (SCR) systems. SCR systems inject a chemical reagent into the flue (exhaust) gas of a NOx producing device, such as a diesel engine or a boiler. The reagent is usually some form of ammonia (aqueous or anhydrous) or aqueous urea. Ammonia (NH_3) reacts with NOx in the presence of a catalyst to produce diatomic nitrogen N_2. Similarly, aqueous urea (CH_4N_2O) evaporates and then gaseous urea decomposes into ammonia which reacts with the NOx. The exact chemical equation depends on which NOx gasses are present, but the products of N_2 and H_2O are much safer than the reactants.

In 2010, the EPA implemented a new standard for diesel engines that required reduced NOx emissions from diesel engines (U.S. Environmental Protection Agency, 2010). SCR systems have become increasingly used to meet the new standard. In order to facilitate the design of SCR systems, it is important that we find a simpler method for modeling the urea evaporation and sublimation chemical processes.

Research Objective

In the summer of 2018, Eldredge and Thomas presented a paper describing how aqueous urea and aqueous ammonia droplets used in Selective Catalytic Reduction (SCR) processes are often modeled as water droplets in an effort to reduce complexity while maintaining accuracy. However, this simplification results in less accurate evaporation rates than a binary component analysis that uses urea or ammonia. To simplify this process, Dr. Eldredge proposed that an equation be developed that accurately reflects urea evaporation, sublimation, and decomposition.

The difficulty with developing this equation is that the usage of urea in SCR processes involves three different phases. First, the water evaporates away from the aqueous urea. Next, the urea sublimates into the gas phase. Finally, in the gas phase, urea decomposes into ammonia, where it can be used in the SCR system to reduce harmful NOx gas emissions.

Based on his research, Dr. Eldredge proposed a general model for an equation that would cover all three stages of urea evaporation and decomposition. Dr. Eldredge and I developed this equation through a multitude of different computer simulations. This paper describes the processes by which we obtained the equation.

ANSYS Testing

Rationale

ANSYS (ANalysis SYStem) is a commonly used software package for computer simulations of fluid flow, heat and mass transfer, and chemical reactions. While it is very powerful, detailed simulations can take a lot of time and computing power to run. In order to simplify calculations, we utilized a simpler and faster program, called Particle. Particle is a Lagrangian based particle tracking program which incorporates heat and mass transfer between discrete and continuous phases. However, we first had to verify the accuracy of the Particle program compared to Fluent, ANSYS' Computational Fluid Dynamics (CFD) Software. To do so, we created a droplet evaporation scenario

Methods

Testing consisted of simulating flow in a 1x1x4 meter duct. One of the square ends of the duct was an inlet, and the other was an outlet. The 4 sides were treated as walls that trapped water droplets that contacted them. Droplets were created near the inlet at the bottom of the duct. Moving air from the inlet pushed the droplets forward through the duct, where they evaporated. Testing required conditions in which the droplets evaporated before the end of the duct and did not contact the walls. A particle track for one of these tests can be seen in Figure 1.

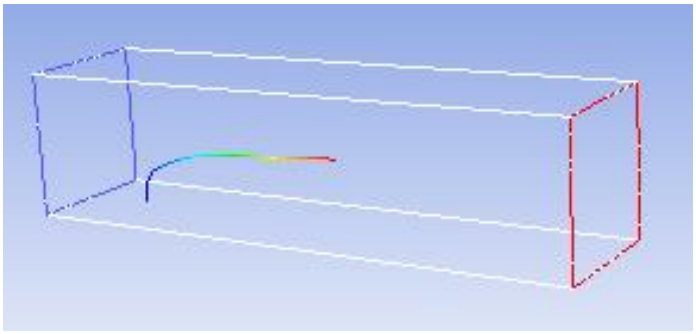

Figure 1. ANSYS particle track of a water droplet evaporating in the SCR duct

Testing

Our first objective was to compare the evaporation of water droplets of varying sizes and temperatures. In their previous work, Eldredge and Thomas (2018) originally evaluated the water droplets in Particle at 3 temperatures (260°C, 316°C, and 427°C) and 3 diameters (50 microns, 100 microns, and 150 microns). Other conditions that remained unchanged through the tests were a gas inlet velocity of 5 m/s, an injector droplet velocity of 50 m/s, and a mass fraction of 0% H2O in the inlet air. We ran 9 simulations with ANSYS Fluent for 1000 iterations each to model each possible combination of temperature and diameter. For the tests, air was used as the continuous phase and water as the discrete phase.

Each of these tests ran smoothly. Each droplet's residence time was plotted against percentage evaporation to see how they evaporated. The plot for a 100-micron drop at 316°C can be seen in Figure 2.

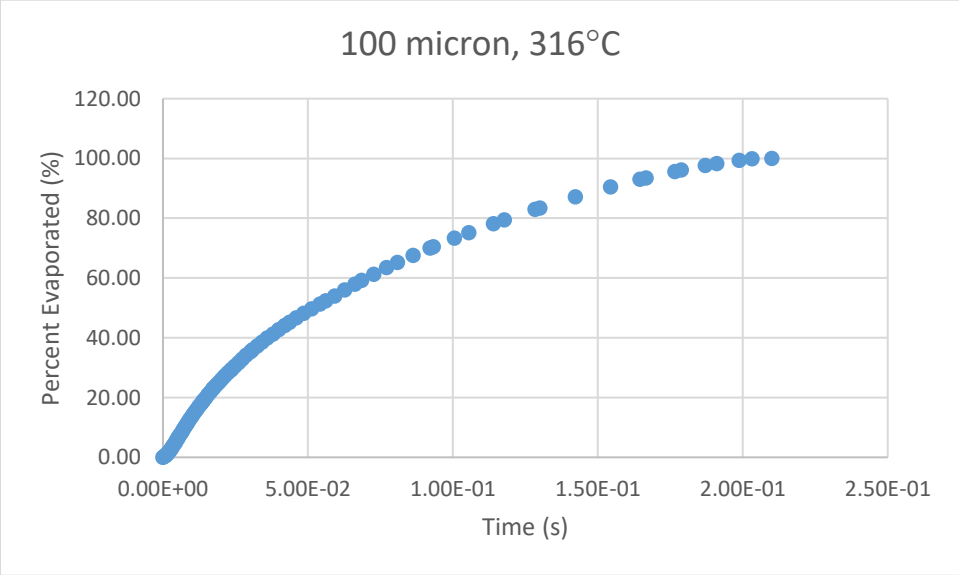

Figure 2. Time vs evaporation percentage for a water droplet with a diameter of 100 microns at a temperature of 316°C

Figure 2 shows that the droplet evaporates much faster at first, and then slower over time. This is due to the changing surface area of the droplet. It starts off at full size, then becomes smaller as it evaporates. The smaller surface area allows less heat transfer, so the remaining water evaporates at a slower rate. All 9 of these tests had similar plots but with different evaporation times.

ANSYS, Particle, and Brin Equation Comparison

With these simulations completed, it was decided to compare evaporation times computed in ANSYS and Particle to Equation 1, developed by A. A. Brin (2009).

$$\tau = \frac{\rho_d \Delta h}{8\lambda_a (T_a)(T_a - T_d)} D_0^2. \quad (1)$$

Where:

τ represents the evaporation time
T_a is the gas temperature
T_d is initial droplet temperature
D_o is the initial diameter of the droplet
Δh is latent heat of vaporization
λ is thermal conductivity of the gas
ρ is density

This indicates that the evaporation time is directly related to the square of droplet diameter and inversely related to the square of gas temperature. We calculated the evaporation times of water droplets under the same conditions that we tested in ANSYS and compared the results. These results can be seen in Table 1. Figures 3 and 4 compare the evaporation times predicted by Particle to ANSYS and the Brin (2009) equation, respectively.

Table 1

Comparison of the Brin equation, ANSYS Fluent, and Particle evaporation times. The symbols next to the diameter show how each size droplet is portrayed on the graphs.

	50 MIC.		●	100 MIC.		▲	150 MIC.		◆
	EQUATION	FLUENT	PARTICLE	EQUATION	FLUENT	PARTICLE	EQUATION	FLUENT	PARTICLE
DEG. 260C	0.0765	0.0928	0.07384	0.3061	0.2719	0.2894	0.6887	0.5725	0.6438
DEG. 316C	0.0573	0.0693	0.05412	0.229	0.2101	0.2109	0.5153	0.4404	0.4678
DEG. 427C	0.0364	0.0421	0.0329	0.1455	0.1368	0.127	0.3274	0.2824	0.2801

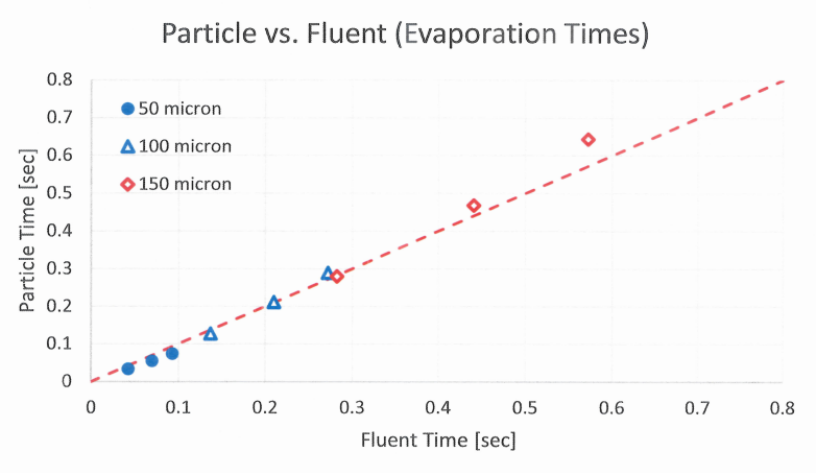

Figure 3. Comparison of evaporation times for ANSYS Fluent and the Particle. The diagonal line represents a 1 to 1 correlation, what the graph should look like if both methods yield the same evaporation time.

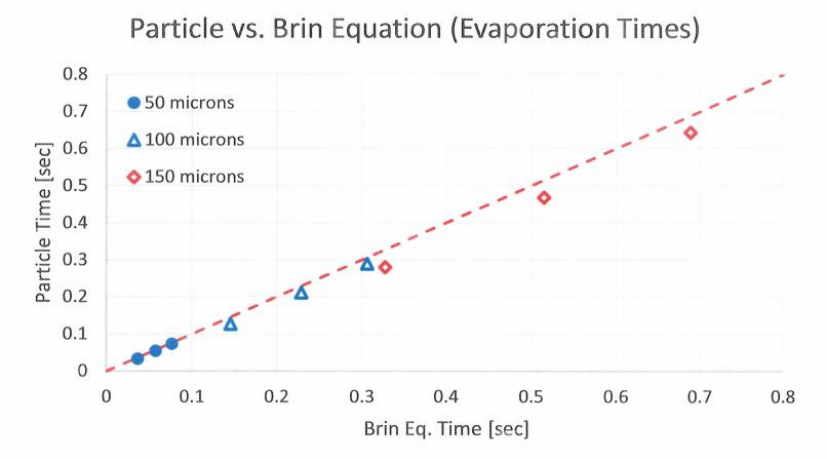

Figure 4. Comparison of evaporation times for Particle and the Brin equation.

Both Figure 3 and 4 as well as Table 1 show that all three methods yield similar results. The times computed by Fluent are similar to the times estimated by Brin's equation, although not close enough to suggest that the results were identical. Compared to the Brin equation, ANSYS slightly underestimated the evaporation times for the 50 micron droplet and overestimated the evaporation times for the 100 and 150 micron droplets.

Low Velocity Testing

To test this, we decided to recreate our ANSYS tests using lower velocities for the gas inlet and the droplet injector to see if the high velocities were affecting the evaporation times. For this set of testing, the gas inlet velocity was changed from 5m/s to .24 m/s and the droplet injector velocity from 50 m/s to .34 m/s. We also changed the temperature range to be from 200°C to 1000°C in increments of 200°C and a droplet diameter of 200 microns. The reasoning for this was to recreate the plot made by Brin in his paper, which uses a similar droplet diameter and temperature distribution.

Unfortunately, ANSYS seemed to have trouble modeling such low velocities. Unlike the smooth, square root-like evaporation graphs that the initial tests created, the low velocity tests created very jagged and irregular graphs. See Appendix for more information.

As the inlet velocity decreased, the graphs begin to behave more and more irregularly. As a result, the low velocity tests were aborted, as they were not considered to be essential to the overall objective.

Particle Reliability Confirmed

Despite the inability of ANSYS to produce realistic results at low velocities, the data generated at higher velocities correlates well with the Particle simulations. Since the Particle simulations of water evaporation correlated closely with both ANSYS results and the empirical equation derived by A.A. Brin (2009), we concluded that it was a valid program for future experiments.

Using Particle to Find Governing Equation

Base Equation

We next ran simulations of the Urea processes using Particle. Particle is able to simulate two of the three processes involved in SCR systems: water evaporation and Urea sublimation. Urea decomposition is governed by chemical kinetics. Future research will incorporate decomposition into Equation 1. Figures 5 and 6 show the evaporation and sublimation processes.

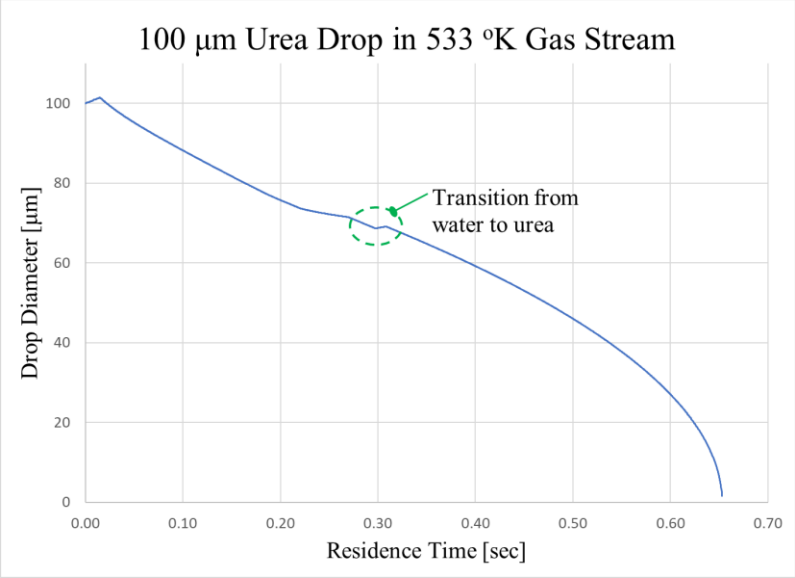

Figure 5. Urea Droplet Diameter versus Time (100 micrometer, 533K gas stream)

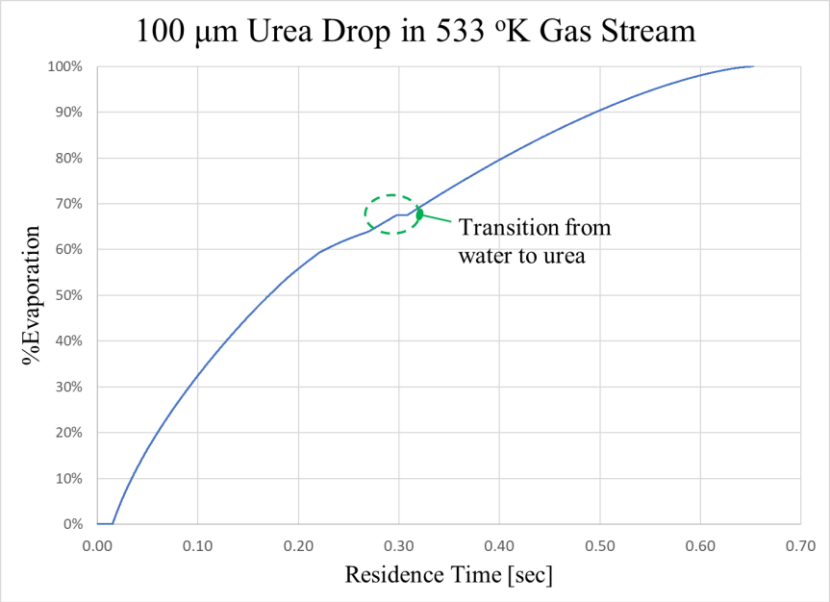

Figure 6. Percent evaporation of urea versus time (100 micrometer, 533K gas stream)

To develop the generic formula for the Urea equation, several plots were generated for water evaporation and urea sublimation at different temperatures. Figures 7-10 show the 4 basic graphs created for tests at each temperature. Each graph from this set was generated using Particle with a gas temperature of 850°F, as the 850°F test was determined to be representative of the population. These graphs relate time t, droplet mass C (where C=100% at time=0), and change in droplet mass over time dC/dt.

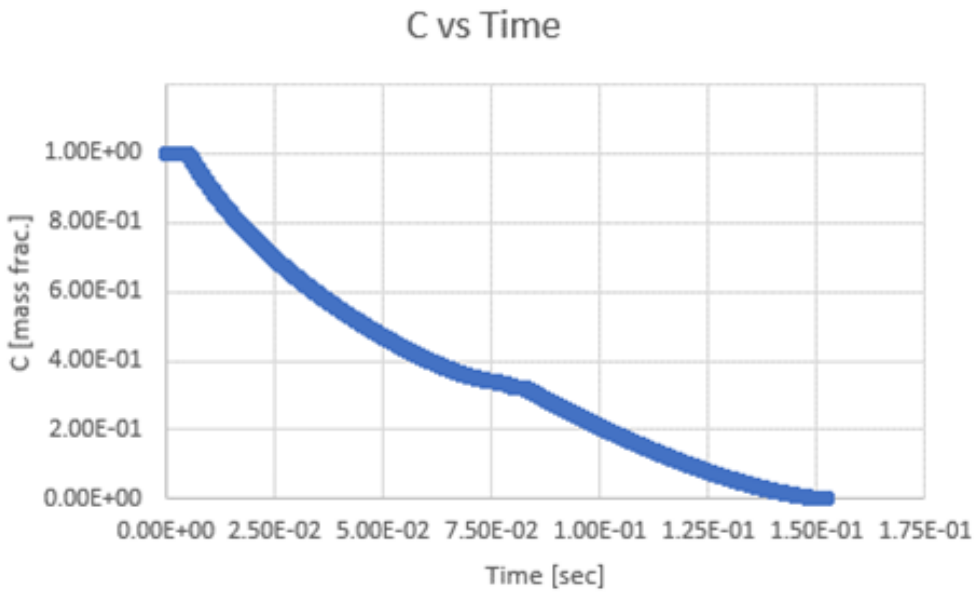

Figure 7. Graph of C versus Time, 850°F (727K)

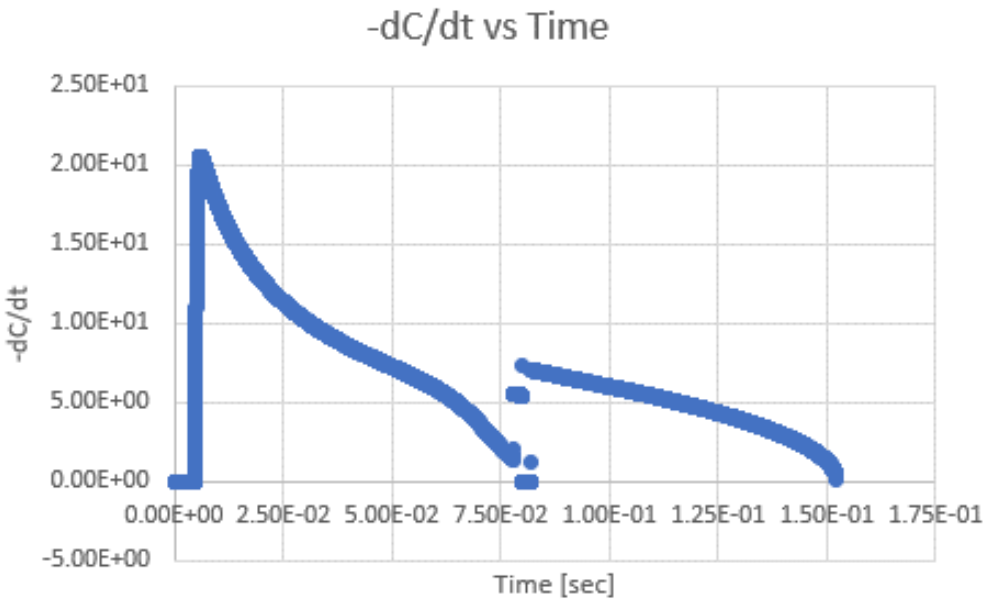

Figure 8. Graph of -dc/dt versus Time, 850°F (727K)

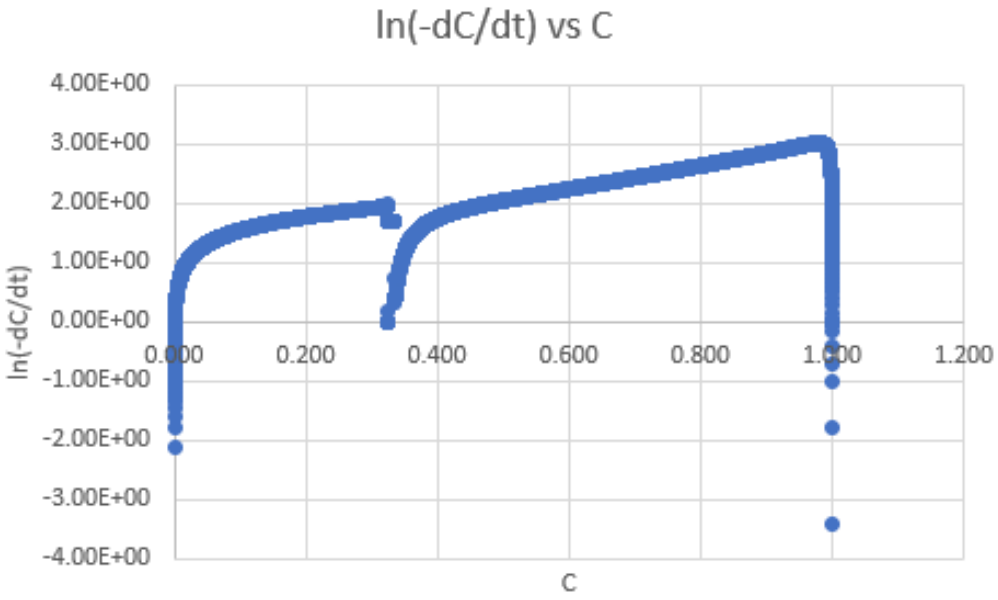

Figure 9. Graph of ln(-dC/dt) versus C, 850°F (727K)

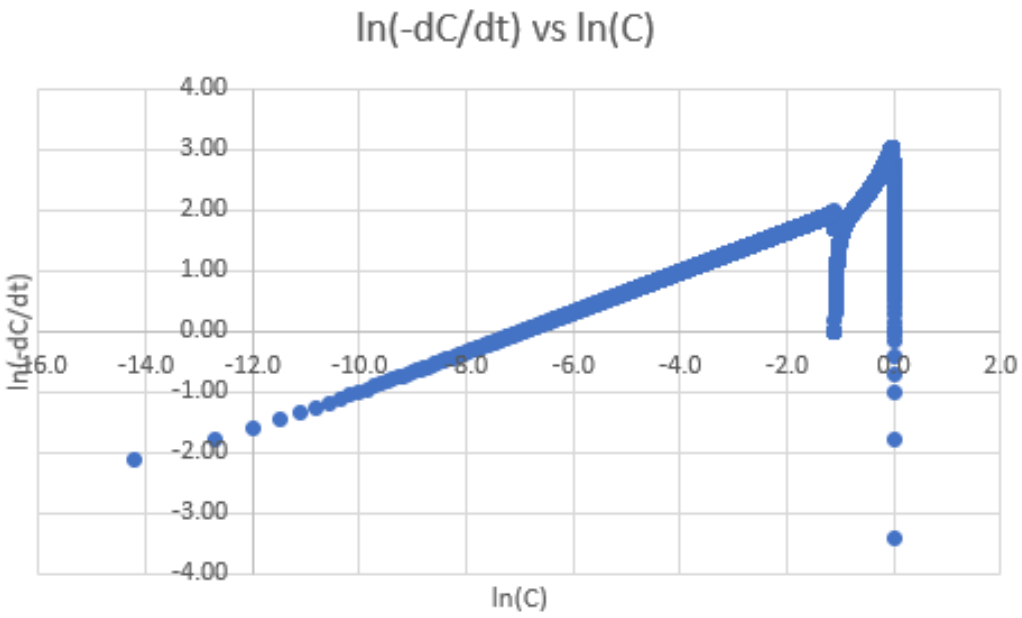

Figure 10. Graph of ln(-dC/dt) versus ln(C), 850°F (727K)

Each graph contains two distinct sections where the data represents different processes. This is based on the first two steps of the urea process. For example, in Figure 7, the water in the solution is evaporating from t=0 to approximately t=8 E-2, at which point the urea begins sublimating.

While the original graph in Figure 7 does not demonstrate a clear mathematical relationship between C and time, Figure 10 shows a nearly linear relationship between the natural logarithms of -dC/dt and C. This relationship is the basis for Equation 2.

Based on the graphical results generated, the proposed Equation 2 has the following form:

$$\frac{dC}{dt} = -C^{n} A\, e^{-\frac{B}{Tg}} \tag{2}$$

Where:

C is nondimensional droplet mass (initially C=1; as the droplet evaporates, C approaches zero)

A is an empirical constant that affects the rate of the evaporation process

B is an empirical constant that incorporates temperature dependence on the evaporation process

n is an empirical exponent that depends on the rate of the evaporation process

T_g is the gas temperature in Kelvin

Taking the natural logarithm of Equation 2 yields:

$$\ln\left(-\frac{dC}{dt}\right) = n \times \ln C + \ln\left[A \times e^{-\frac{B}{Tg}}\right] \tag{3}$$

Equation 3 is shown to be linear with the following variables:

$$y = \ln\left(-\frac{dC}{dt}\right) \tag{4}$$

$$x = \ln C \tag{5}$$

$$b = \ln\left[A \times e^{\frac{-B}{Tg}}\right] \tag{6}$$

Equation 2 then becomes Equation 7:

$$y = nx + b \tag{7}$$

This basic linear formula is represented by the graph shown in Figure 10. The goal is to find appropriate values for n, A, and B that would complete this equation and accurately represent the urea processes of evaporations and sublimation for SCR applications. It was decided to let A=1. For future work, A would represent the effect of Urea decomposition.

Additionally, the evaporation time can be found by integrating Equation 2:

$$\int_1^C C^{-n} dC = -e^{\left(-\frac{B}{Tg}\right)} \tag{8}$$

$$\frac{C^{1-n} - 1}{1 - n} = -e^{-\frac{B}{Tg}} t \tag{9}$$

$$t_{evap} = \frac{1 - C_{evap}^{1-n}}{-(1-n)e^{-\frac{B}{Tg}}} \tag{10}$$

Where C_{evap} = 0.001 indicating that the droplet has 0.1% of its original mass.

Urea Evaporation and Sublimation

To find the values for the unknown constants in this equation, a larger sample of data was collected. To do this, we ran simulations of aqueous urea in high temperature gas streams in

Particle. The temperatures we tested ranged from 400°F (477.6K) to 980°F (800.0K). This temperature range is inclusive of most SCR applications.

For temperatures at and above 600°F, the simulation performed as expected. The graphs appeared similar to the ones produced for 850°F, with decreasing evaporation times as the temperature increased. However, the 400°F and 500°F plots of ln(-dc/dt) exhibited unusual behavior, which is believed to be an anomaly associated with the calculation of dc/dt. Every few data points, the value of C would drop by approximately 2-3 times as much as it had over the previous timestep. This meant that the dC/dt value had several radical outliers. Table 2 shows a section of the data generated by Particle at 400°F. Approximately every 25 time steps, the value of C would experience a much larger drop than the step before. This resulted in the much smaller dC/dt value, as can be seen highlighted in the table.

As expected, this data yielded graphs that were similarly bizarre. While the data jumps represented anomalies, the total times for evaporation appeared accurate. A filtering program was used that removed all the data points that had a significantly different dC/dt value than the one before it. The data for both the 400°F and the 500°F tests were filtered. This yielded the same total evaporation time with a much more realistic curve of data points. Figure 11 demonstrates the effectiveness of this process with a comparison of the ln(-dC/dt) versus ln(C) graphs for 600°F (lowest temperature with realistic data), 400°F without filtering, and 400°F with filtering during the interval of water evaporation.

Table 2

A section of the data from the 400F simulation

ln(-dC/dt)	-dC/dt	C	ln(C)
6.31E-01	1.88E+00	8.1254E-01	-0.20759
6.31E-01	1.88E+00	8.1250E-01	-0.20764
6.31E-01	1.88E+00	8.1247E-01	-0.20768
6.33E-01	1.88E+00	8.1243E-01	-0.20773
6.31E-01	1.88E+00	8.1239E-01	-0.20777
6.31E-01	1.88E+00	8.1235E-01	-0.20782
6.31E-01	1.88E+00	8.1232E-01	-0.20787
6.31E-01	1.88E+00	8.1228E-01	-0.20791
-5.99E-02	9.42E-01	8.1226E-01	-0.20794
6.31E-01	1.88E+00	8.1222E-01	-0.20798
6.31E-01	1.88E+00	8.1218E-01	-0.20803
6.31E-01	1.88E+00	8.1215E-01	-0.20807
6.30E-01	1.88E+00	8.1211E-01	-0.20812
6.31E-01	1.88E+00	8.1207E-01	-0.20817
6.31E-01	1.88E+00	8.1203E-01	-0.20821
6.31E-01	1.88E+00	8.1200E-01	-0.20826
6.31E-01	1.88E+00	8.1196E-01	-0.20831
6.31E-01	1.88E+00	8.1192E-01	-0.20835
6.29E-01	1.88E+00	8.1188E-01	-0.2084
6.31E-01	1.88E+00	8.1185E-01	-0.20844
6.31E-01	1.88E+00	8.1181E-01	-0.20849
6.29E-01	1.88E+00	8.1177E-01	-0.20854
6.32E-01	1.88E+00	8.1173E-01	-0.20858
6.31E-01	1.88E+00	8.1170E-01	-0.20863
6.29E-01	1.88E+00	8.1166E-01	-0.20868
6.31E-01	1.88E+00	8.1162E-01	-0.20872
6.29E-01	1.88E+00	8.1158E-01	-0.20877
6.31E-01	1.88E+00	8.1155E-01	-0.20881
6.29E-01	1.88E+00	8.1151E-01	-0.20886
6.32E-01	1.88E+00	8.1147E-01	-0.20891
6.29E-01	1.88E+00	8.1143E-01	-0.20895
6.31E-01	1.88E+00	8.1140E-01	-0.209
-6.41E-02	9.38E-01	8.1138E-01	-0.20902
6.29E-01	1.88E+00	8.1134E-01	-0.20907

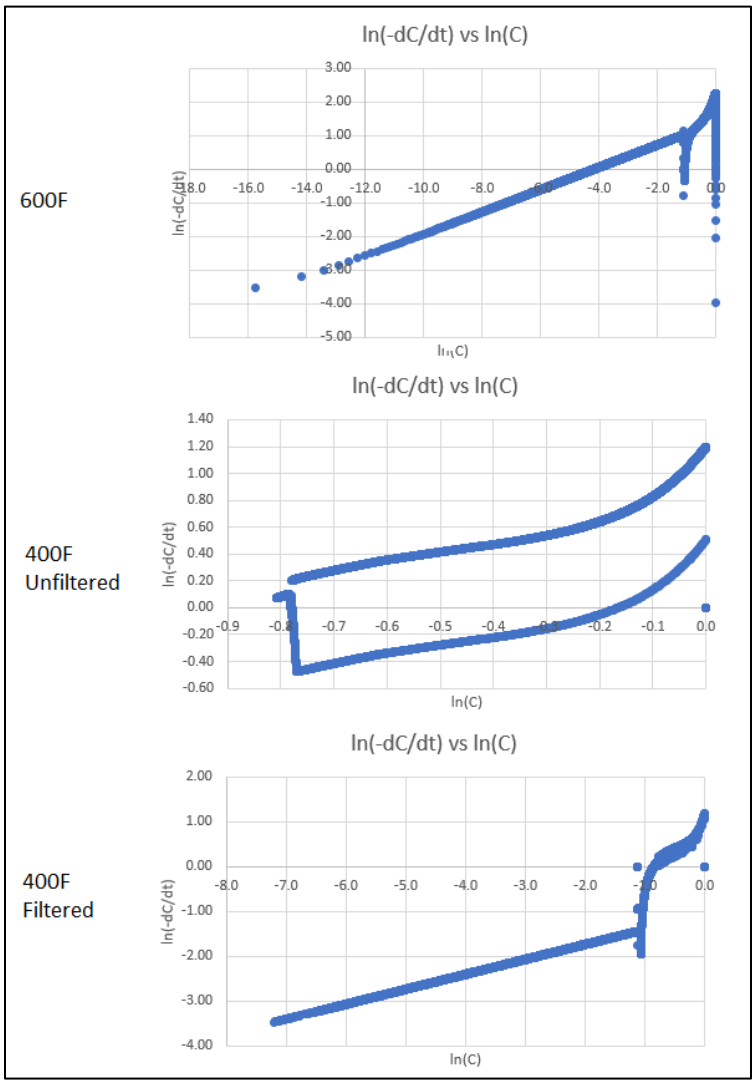

Figure 11. Comparison of ln(-dC/dt) versus ln(C) graphs for 600F, 400F unfiltered, and 400F filtered

The results of the tests conducted in Particle are tabulated in Table 3. In reference to Figure 11, n is the slope of the line in the ln(-dC/dt) versus ln(C) graph. The line on the left-hand side of these graphs represents urea sublimation while the line on the right represents water evaporation. Chronologically, these graphs go from right to left. The time listed is the total time needed for the water to evaporate and the urea to sublimate at the given temperature.

Table 3

Results of water evaporation and urea sublimation in particle (gas temperature range 600F to 980F)

T_g (F)	T_g (K)	D (μm)	V (ft/s)	n water	n urea	Time(sec)
600	589	40	16.4	1.352192	0.331172	0.05915
700	644	40	16.4	1.379008	0.332455	0.039827
800	700	40	16.4	1.385791	0.331431	0.02916
900	755	40	16.4	1.385002	0.331786	0.022474
980	800	40	16.4	1.380992	0.332283	0.018736
600	589	40	40	1.354918	0.331264	0.05911
700	644	40	40	1.383656	0.331936	0.039795
800	700	40	40	1.390267	0.330925	0.029124
900	755	40	40	1.389486	0.331891	0.022446
980	800	40	40	1.385191	0.332143	0.018713
600	589	80	16.4	1.499072	0.333059	0.232376
700	644	80	16.4	1.57236	0.333959	0.155467
800	700	80	16.4	1.527669	0.332128	0.113176
900	755	80	16.4	1.513146	0.333146	0.08673
980	800	80	16.4	1.503617	0.33485	0.07201
600	589	80	40	1.503756	0.333177	0.23222
700	644	80	40	1.577823	0.333894	0.15534
800	700	80	40	1.53165	0.331993	0.113056
900	755	80	40	1.518253	0.332141	0.08665
980	800	80	40	1.508109	0.333936	0.07191
600	589	100	16.4	1.542465	0.333260	0.360959
700	644	100	16.4	1.579462	0.333094	0.241002
800	700	100	16.4	1.595491	0.332565	0.175072
900	755	100	16.4	1.587850	0.333840	0.133957
980	800	100	16.4	1.574229	0.335756	0.111031
600	589	100	40	1.543179	0.333313	0.360748
700	644	100	40	1.674841	0.332871	0.240812
800	700	100	40	1.601482	0.332568	0.174894
900	755	100	40	1.592744	0.333699	0.133797
980	800	100	40	1.564146	0.335098	0.110880
600	589	130	16.4	1.582511	0.333762	0.605895
700	644	130	16.4	1.678558	0.333611	0.403591
800	700	130	16.4	1.58998	0.333293	0.292498
900	755	130	16.4	1.567577	0.334995	0.223268
980	800	130	16.4	1.537421	0.336757	0.184726
600	589	130	40	1.585109	0.330688	0.60567
700	644	130	40	1.727524	0.33348	0.403268
800	700	130	40	1.665789	0.333417	0.292188
900	755	130	40	1.665544	0.335107	0.222974
980	800	130	40	1.655174	0.336866	0.18445
600	589	160	16.4	1.60476	0.333391	0.913062
700	644	160	16.4	1.718819	0.333725	0.607021
800	700	160	16.4	1.711919	0.333992	0.439047
900	755	160	16.4	1.716655	0.335604	0.33452
980	800	160	16.4	1.707755	0.337739	0.276373
600	589	160	40	1.608056	0.332471	0.912318
700	644	160	40	1.722857	0.333621	0.606543
800	700	160	40	1.71541	0.334019	0.438613
900	755	160	40	1.72147	0.335635	0.334116
980	800	160	40	1.71229	0.337752	0.275984

To ensure a wide range of data, we ran these tests for droplets with 5 different diameters (40, 80, 100, 130, 160 microns) and 2 different gas velocities (16.4 and 40 ft/s). Each test consisted of running a particle simulation at 600°F, 700°F, 800°F, 900°F, and 980°F. Subsequent analysis revealed that gas velocity only had a minor effect on evaporation time. Conversely, gas temperature and drop diameter both significantly affected the evaporation time.

Urea Decomposition

We evaluated the decomposition time of urea. The chemical reaction for urea decomposition is as follows (Yim et al., 2004):

$$(NH_2)_2CO \rightarrow NH_3 + HNCO$$

In the presence of a catalyst in a selective catalytic reactor, the HNCO (isocyanic acid) will hydrolyze according to the reaction:

$$HNCO + H_2O \rightarrow NH_3 + CO_2$$

The NH_3 (Ammonia) created by this process reduces Nitrous Oxides (NO_x) molecules in the Selective Catalytic Reactor (SCR).

The decomposition reaction was modeled using chemical kinetic calculations. Urea was considered to be decomposed when 99.9% had undergone decomposition. The decomposition of Urea was computed as a function of time. Linear interpolation was used to find at what time 99.9% was decomposed and plotted the results, as seen in Figure 12. These results were compared to the decomposition times found by Eldredge and Thomas (2018) to confirm their reliability.

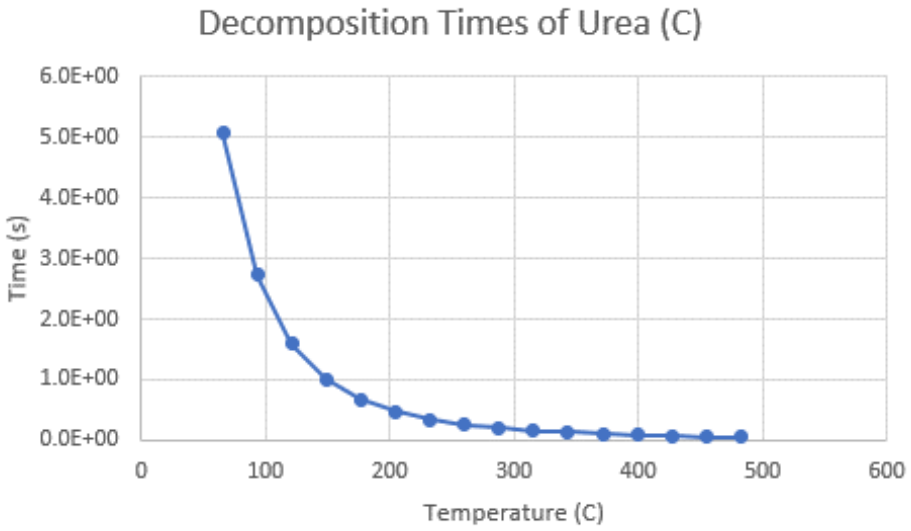

Figure 12. Decomposition time of urea versus temperature

With the values for water evaporation, urea sublimation, and urea decomposition all found, a table was made that included all of this data for the 100 micron tests (Table 4). Note, the evaporation times in Table 4 include both water evaporation and Urea sublimation.

Table 4

Summary of Particle and Chemkit results

Temp (F)	Temp (K)	n water	n urea	Weight urea	n average	b	B	Evap Time	Decomp Time
400	477.59	2.0630816	0.334165	0.839080904	0.612380737	1.1877	-567.239	2.67E+00	4.71E-01
500	533.15	1.396996	0.334226	0.329435804	1.046881642	1.864238	-993.919	6.24E-01	2.57E-01
600	588.71	1.5424645	0.33326	0.472014633	0.971702312	2.268289	-1335.35	3.61E-01	1.58E-01
700	644.26	1.579462	0.333094	0.421095186	1.05462225	2.62362	-1690.3	2.41E-01	1.06E-01
750	672.04	1.5913113	0.332501	0.39717608	1.091341972	2.771008	-1862.22	2.04E-01	8.89E-02
800	699.82	1.5954912	0.332565	0.376956562	1.119422701	2.903391	-2031.84	1.75E-01	6.48E-02
850	727.59	1.595584	0.333092	0.354695687	1.14778359	3.023692	-2200.02	1.52E-01	5.58E-02
900	755.37	1.5878497	0.33384	0.331648021	1.171959978	3.133598	-2367.03	1.34E-01	4.86E-02
avg		1.61903	0.333343		1.086244921				

The future goal is to incorporate decomposition into Equation 1 in order to account for all 3 processes of the SCR process. However, the work presented here only describes the water evaporation and urea sublimation processes.

Discussion

The constant b in Table 4 is the y intercept of the ln(-dC/dt) versus ln(C) plot as described by Equation 7. The value for b was taken from ln(-dC/dt) versus ln(C) data plots like the one from Figure 10. The constant b is based on a logarithmic function and ln(C) equals zero at time equals zero. We used the maximum height of the graph as an approximation for the intercept since this point occurs at the lowest time on the linear portion of the graph and is therefore close to what the intercept would be.

B (from Table 4) is one of the unknown constants from Equation 1. We calculated it by allowing A=1. With this assumption, Equation 6 simplifies to:

$$b = -\frac{B}{T_g} \tag{11}$$

Notably, the 400°F and 500°F results have significantly different values for the slope of water (n water) than the other tests. The reason for these differences is unknown at this time. The decision was made to disregard the entire data set for the 400°F and 500°F tests.

By substituting in all these values, the differential Equation 12 is created.

$$\ln\left(-\frac{dC}{dt}\right) = n \times \ln C - \frac{B}{T_g} \tag{12}$$

Interestingly, the results of our analysis did not yield a constant value for B, but rather linear relationship with gas temperature. This relationship is demonstrated for the 100 micron 16.4 ft/s test in Figure 13.

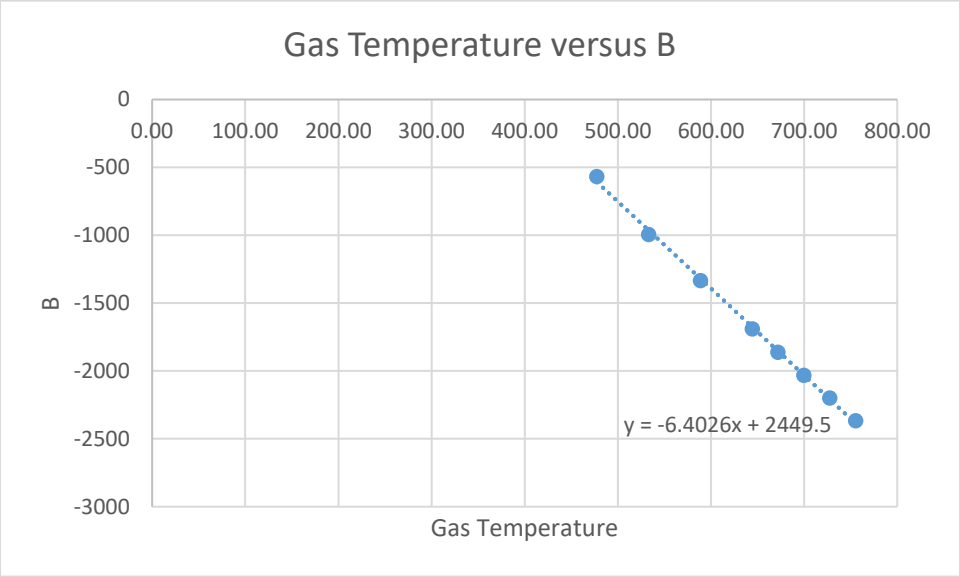

Figure 13. The Linear relationship of B Compared to Gas Temperature

These values, along with those generated by the other sizes and speeds, provide values for the following substitution (Equation 13):

$$B = mT_g - T_{gi} \tag{13}$$

Where T_g is the gas temperature as before, m is the slope of the calculated B values relative to T_g, and T_{gi} is the intercept created in Figure 13. The averages from the full set of m and T_{gi} values calculated are as follows in Table 5.

Table 5

Calculated m and Tgi for each size and gas velocity

Gas Velocity (ft/s)	Size (Microns)	m	T_{gi} (intercept)
16.4	40 mic	-7.6519	2188.3
16.4	80 mic	-6.4998	2247.5
16.4	100 mic	-6.4026	2449.5
16.4	130 mic	-6.157	2654.1
16.4	160 mic	-5.3922	2329.8
40	40 mic	-7.6592	2189.9
40	80 mic	-6.5807	2249.9
40	100 mic	-6.149	2274.4
40	130 mic	-5.7312	2306.8
40	160 mic	-5.4028	2333.3
average		-6.36264	2322.35

This yields Equations 14 and 15 as follows:

$$\ln\left(-\frac{dC}{dt}\right) = n \times \ln C - \frac{-6.36264T_g + 2322.35}{T_g} \tag{14}$$

$$t_{evap} = \frac{1 - C_{evap}^{(1-n)}}{(1-n)e^{\frac{6.36264Tg - 2322.35}{Tg}}} \tag{15}$$

Analysis of the data generated by Equation 15 revealed that the droplet evaporation and sublimation times had a dependence on the initial droplet diameter $D_{o,}$ similar to Equation 1

(Brin, 2009). Figure 14 shows the evaporation and sublimation times predicted by Equation 15 compared to Particle's times.

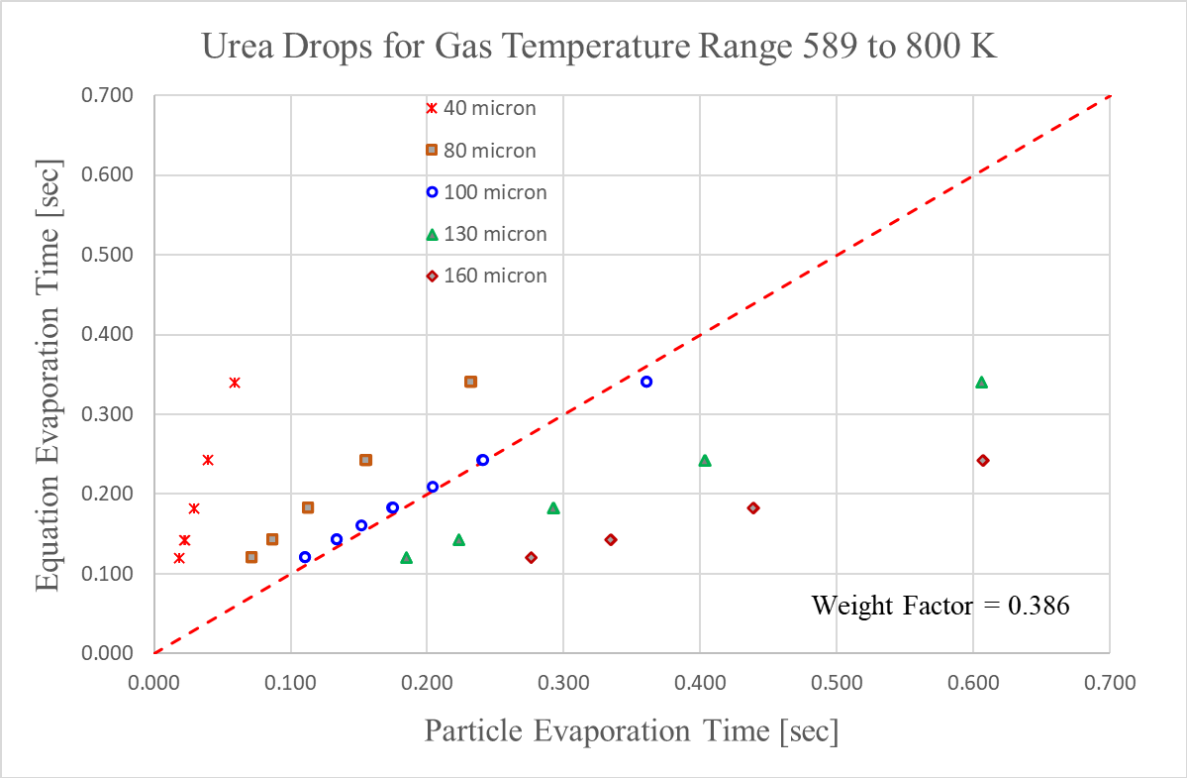

Figure 14. Particle versus equation evaporation times

Modifying Equations 2 and 15 to account for initial diameter yields the following:

$$\frac{dC}{dt} = -C^n \left(\frac{D_o}{100}\right)^{-2} e^{\frac{6.36264Tg-2322.35}{Tg}} \tag{16}$$

$$t_{evap} = \frac{\left(1 - C_{evap}^{(1-n)}\right) \times \left(\frac{D_o}{100}\right)^2}{(1-n)e^{\frac{6.36264Tg-2322.35}{Tg}}} \tag{17}$$

In equations 16 and 17, D_o is the initial droplet diameter in units of µm.

The final step was to calculate the value of the parameter n. Values of n were determined for both water evaporation and urea sublimation (n water and n urea). These values were weighted to find an overall value of n using Equation 18.

$$n = n_{urea}\,(1 - W_f) + n_{water}\,W_f \tag{18}$$

By substituting in a range of W_f values, the deviation of Equation 17 versus Particle evaporation and sublimation times could be plotted (see Figure 15).

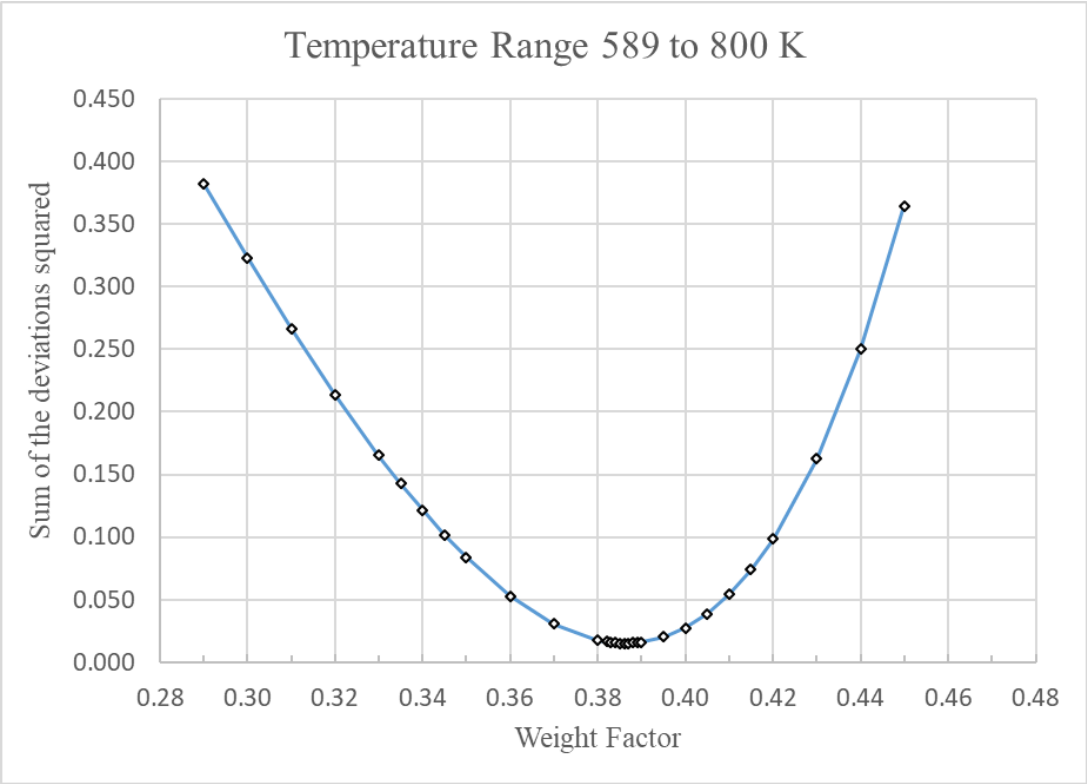

Figure 15. Deviation between Equation 10 and Particle by weight factor

Figure 15 shows that the ideal weight factor (where the deviation is minimal) occurs for a value of W_f around 0.386. Using this value, n equals 1.47580. This creates final Equations 19 and 20.

$$\frac{dC}{dt} = -C^{1.47580} \times \left(\frac{D_0}{100}\right)^{-2} * e^{\frac{6.36264Tg - 2322.35}{Tg}} \tag{19}$$

$$t_{evap} = \frac{\left(1 - C_{evap}^{(-0.47580)}\right) \times \left(\frac{D_o}{100}\right)^2}{(0.47580)e^{\frac{6.36264Tg - 2322.35}{Tg}}} \tag{20}$$

Equation 20 is plotted against particle evaporation times to show the equation's accuracy in Figure 16.

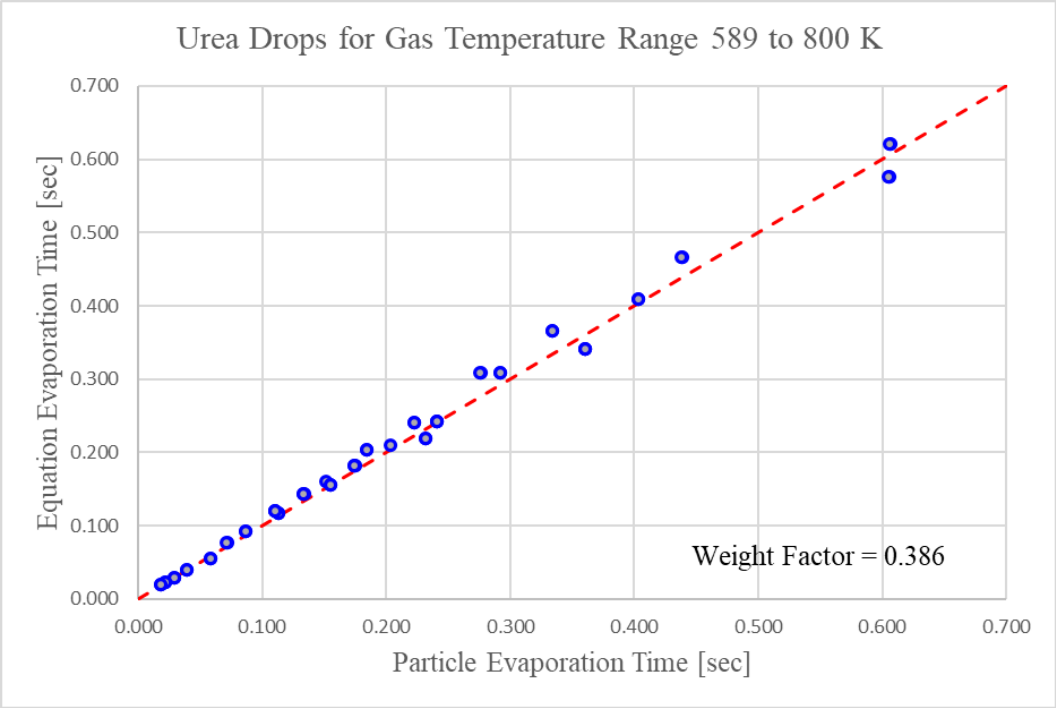

Figure 16. Evaporation times for Particle versus Equation 17

Conclusions

The result of our tests was a differential equation that approximately describes the time it takes the water in aqueous urea to evaporate and the urea to sublimate. This equation, combined with previously developed equations for fluid evaporation, could be used to fully define the SCR process. Equation 12 could easily be implemented into computational fluid dynamics (CFD) software, which would significantly simplify urea evaporation and sublimation.

Unfortunately, this equation does not implement the simulated results for Urea decomposition. For future work, I would recommend finding a means of adding this to the equation.

References

Abu-Ramadan, E., Saha, K., & Li, X. (2011). Modeling the depleting mechanism of urea-water-solution droplet for automotive selective catalytic reduction systems. *AIChE Journal*, *57*(11), 3210-3225. doi:10.1002/aic.12523

Benjamin, S., & Roberts, C. (2012). Significance of droplet size when injecting aqueous urea into a selective catalytic reduction after-treatment system in a light-duty diesel exhaust. *Fuel Systems for IC Engines*, 43-60. doi:10.1533/9780857096043.2.43

Bernhard A.M., Czekaj I., Elsener M., Wokaun A., & Kröcher, O. (2011) Evaporation of urea at atmospheric pressure *The Journal of Physical Chemistry 115*(12), 2581-2589 DOI: 10.1021/jp112066m

Birkhold, F., Meingast, U., Wassermann, P., & Deutschmann, O. (2006). Analysis of the injection of urea-water-solution for automotive SCR denox-systems: Modeling of two-phase flow and spray/wall-interaction. *SAE Technical Paper Series*. doi:10.4271/2006-01-0643

Brin, A. A. (2009, May). Evaporation of water droplets in a high temperature gas flow. *ResearchGate.*

Eldredge, T., & Thomas, M. (2018). Investigation of the evaporation processes for aqueous ammonia and aqueous urea and guidelines for using simplifying assumptions. *American Society of Mechanical Engineers.* doi:10.1115/power2018-7218

Environmental Protection Agency **(**2015**).** *Selective Catalytic Reduction***.** Retrieved from http://https://www3.epa.gov/ttnecas1/models/SCRCostManualchapter_Draftforpubliccomment6-5-2015.pdf

Faltsi, R., & Mutyal, J. (2012, October). Confidence in modeling SCR aftertreatment systems. *Automotive Simulation World Conference.*

Ganesh, S. & Srinivas, T. (2017). Development of thermo-physical properties of aqua ammonia for Kalina cycle system. nt. J. *Materials and Product Technology*. *55*. 113-140.

Holterman, H.J. (2003). Kinetics and evaporation of water drops in air. *IMAG Report.*

Kayser, R., & Bennett, H. S. (1977). Evaporation of a liquid droplet. journal of research of the national bureau of standards. *Physics and Chemistry*, *81A*(2/3), 257. doi:10.6028/jres.081a.015

Majewski, W. A. (n.d.). Urea dosing and injection systems. Retrieved from https://www.dieselnet.com/tech/cat_scr_mobile_urea_dosing.php

Miliauskas, G., & Sabanas, V. (2017). Interacting heat transfer processes in water droplets. *Mechanika 52*(2) 17-27 Retrieved from http://mechanika.ktu.lt/index.php/Mech/article/view/13006

Nishad, K., Sadiki, A., & Janicka, J. (2018). Numerical investigation of adblue droplet evaporation and thermal decomposition in the context of NOx-SCR using a multi-component evaporation model. *Energies*, *11*(1), 222. doi:10.3390/en11010222

NIST Chemistry WebBook. (n.d.). Retrieved from https://webbook.nist.gov/chemistry/

Schading, G., Luijten, C., & Roth, P. (1995). Sublimation of urea particles at high temperatures. *Journal of Aerosol Science*, *26*(1), S221-S222. doi:10.1016/0021-8502(95)97018-a

U.S. Environmental Protection Agency, (2010). Available and emerging technologies for reducing greenhouse gas emissions from coal-fired electric generating units. Retrieved

from https://www.epa.gov/sites/production/files/2015-12/documents/electricgeneration.pdf

Wang, T. J., Baek, S. W., Lee, S. Y., Kang, D. H., & Yeo, G. K. (2011). Evaporation characteristics of ammonium formate-urea-water solution droplet for SCR systems. *Advanced Materials Research*, 415-417, 2252-2256. doi:10.4028/www.scientific.net/amr.415-417.2252

What is Acid Rain? (2019, January 28). Retrieved from https://www.epa.gov/acidrain/what-acid-rain

Yim, S.D., Kim, S.J., Baik, J.H., Nam, I.S., Mok, Y.S., Lee, J.H.… Oh, S.H. (2004). Decomposition of urea into NH3 for the SCR process. *Industrial & Engineering Chemistry Research 43*(16), 4856-4863. DOI: 10.1021/ie034052j

Appendix

As can be seen from Figures A1-A3, the evaporation plots seem very inaccurate. Figure A1 seems to indicate that the droplet stopped evaporating for nearly a full second before quickly evaporating over the next half-second. Figure A2 was the most like the original data set, but still seemed much too irregular to be accurate. Figure A3 has a mix of plateaus and curves, with seemingly no pattern.

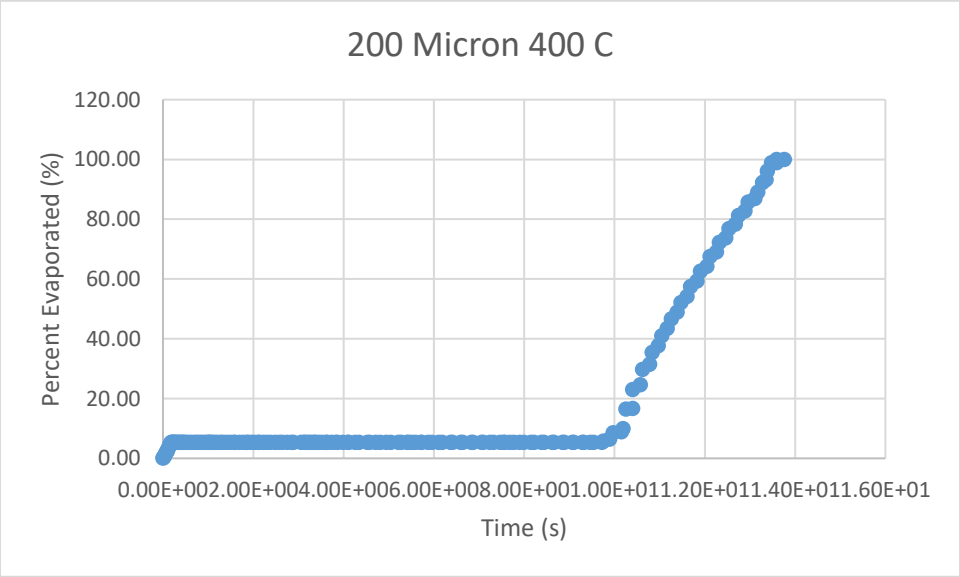

Figure A1. Low velocity evaporation plot for 200 micron, 400C droplet

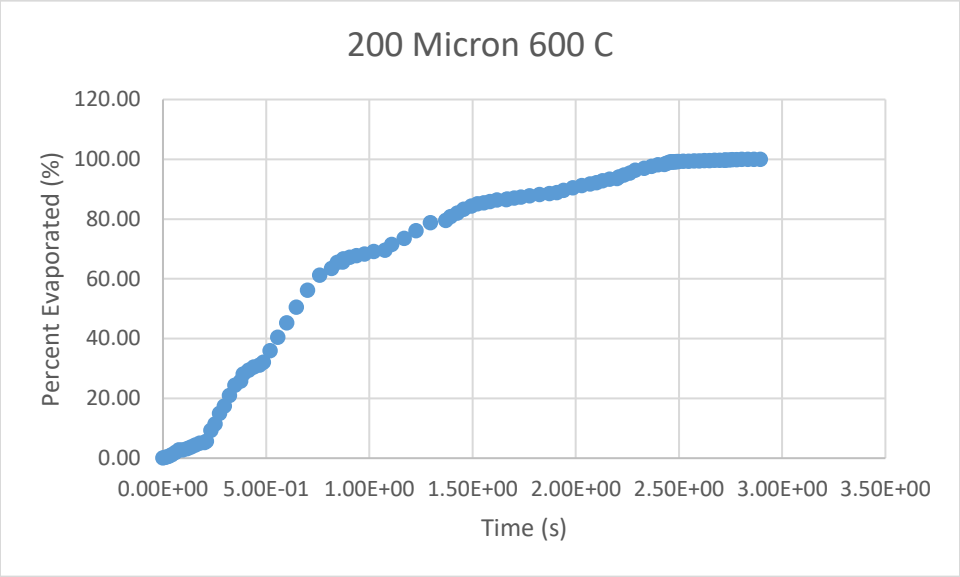

Figure A2. Low velocity evaporation plot for 200 micron, 600C droplet. This was the most regular looking graph out of the lot.

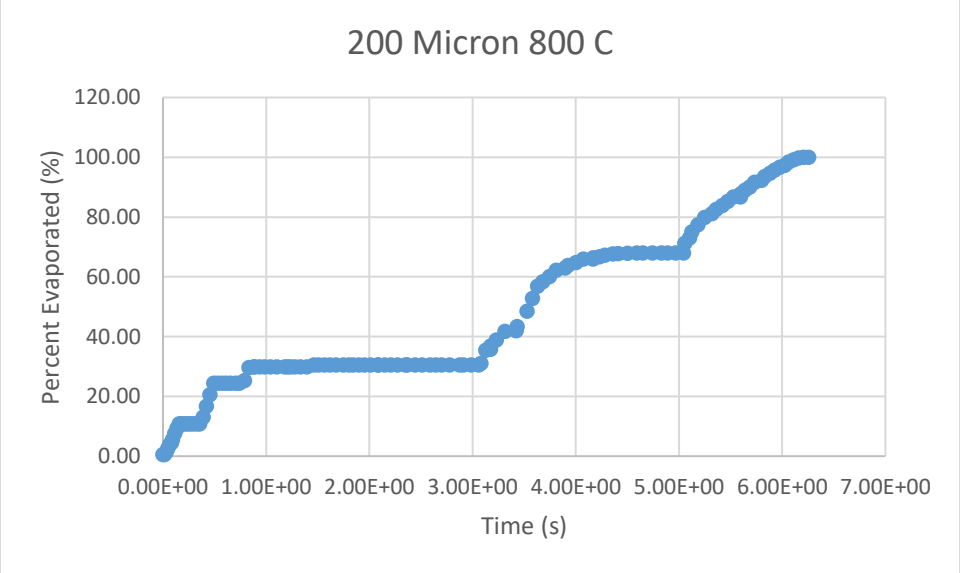

Figure A3. Low velocity evaporation plot for 200 micron, 800C droplet

We determined that the results were inaccurate because ANSYS' calculations did not converge. ANSYS simulates these models using an iterative process. Over a few hundred or thousand iterations, the model's residuals should converge to very low values. The lower the

residuals, the more accurate the numbers should be. Figure A4 demonstrates a normal plot of a simulation's residuals versus the number of iterations performed.

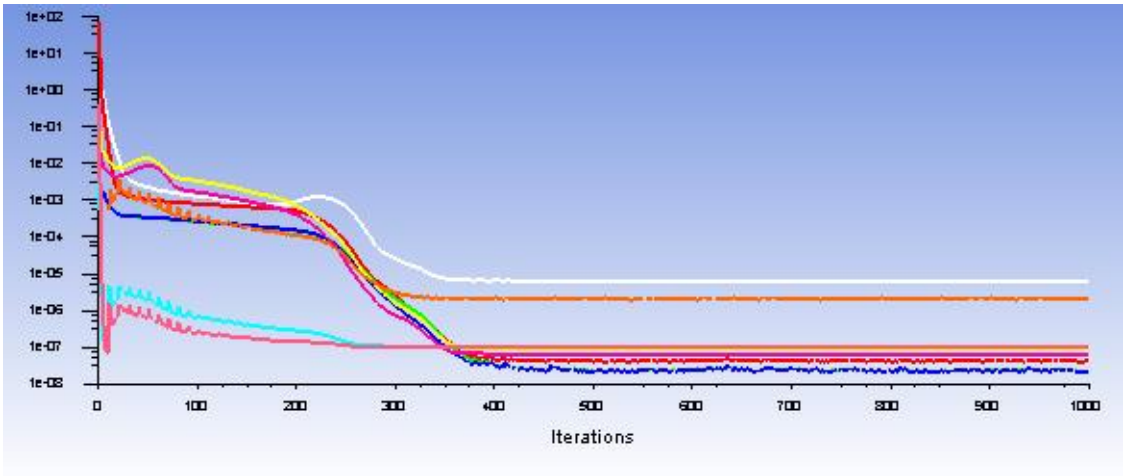

Figure A4. A normal plot of the residuals from an ANSYS simulation

While the residuals may oscillate in some of the earlier iterations, they will converge after a few hundred, and remain almost unchanged after 500 iterations. After this point, most of them stay below 10^{-7} and the highest only reach 10^{-5}. All of my original tests in ANSYS demonstrated a similar pattern with their residuals. The low velocity tests did not replicate this plot. Figures A5 and A6 show the residuals for a low velocity test.

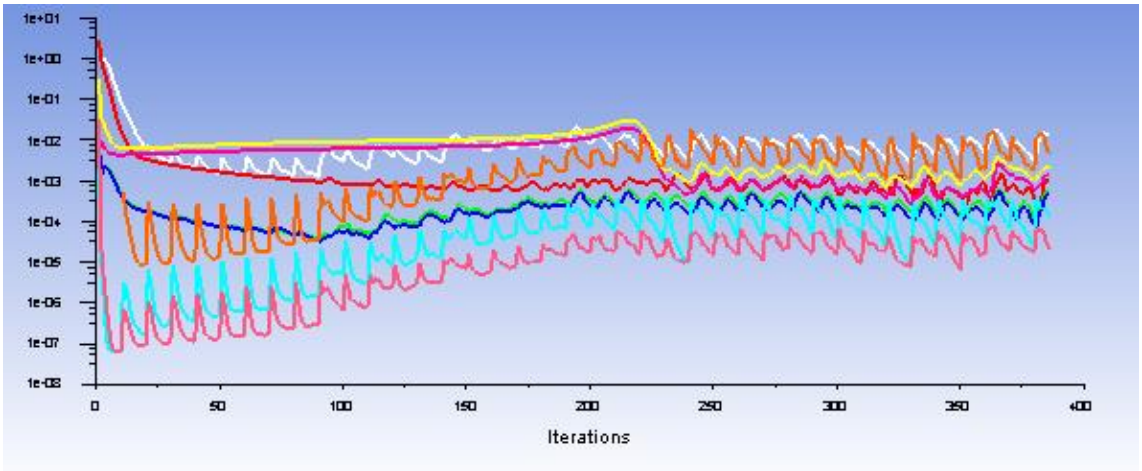

Figure A5. Low velocity residual plot after nearly 400 iterations

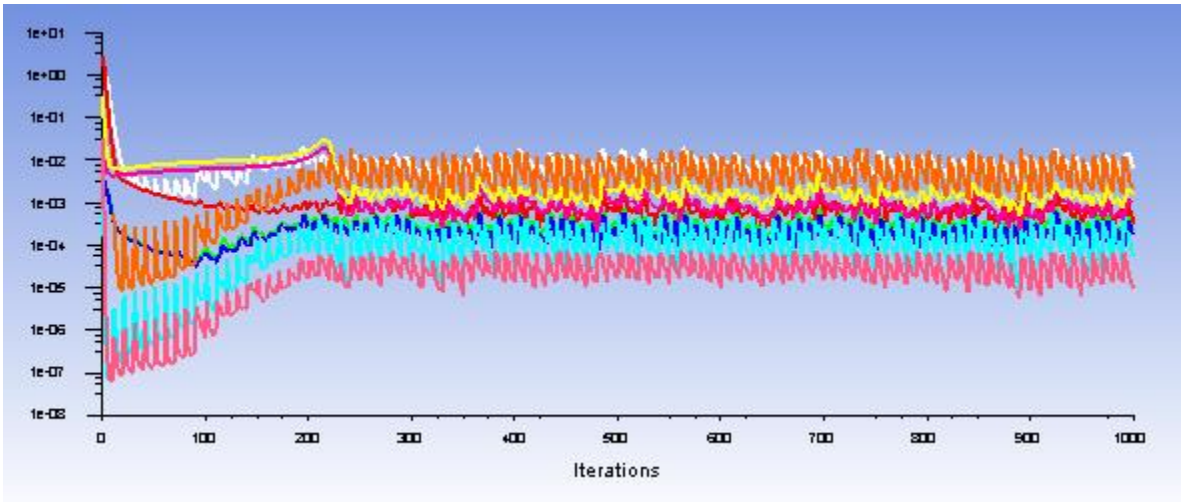

Figure A6. Low velocity residual plot after a full 100 iterations.

As can be seen by these plots, the residuals of the low velocity tests never converge. In fact, they increase after the first 200 iterations, only to continually oscillate afterwards. They are also quite high, with a low end of around 10^{-5} after the initial rise and a high end of over 10^{-2}. The fact that these residuals are so high partially explains why the results are so inaccurate.

We decided to find out how the changing velocities affected ANSYS' ability to converge to a solution. Tests were run with an injector velocity of 5m/s and varying gas velocities of 2, 1, and 0.5 m/s. The results showed a clear trend. The lower the gas velocity, the further the graph shifted from the standard evaporation curve. Figures A8-10 show the evaporation plots of these 3 new tests along with the evaporation plot of a standard simulation (Figure A7) and a very low velocity test (Figure A3, repeated)

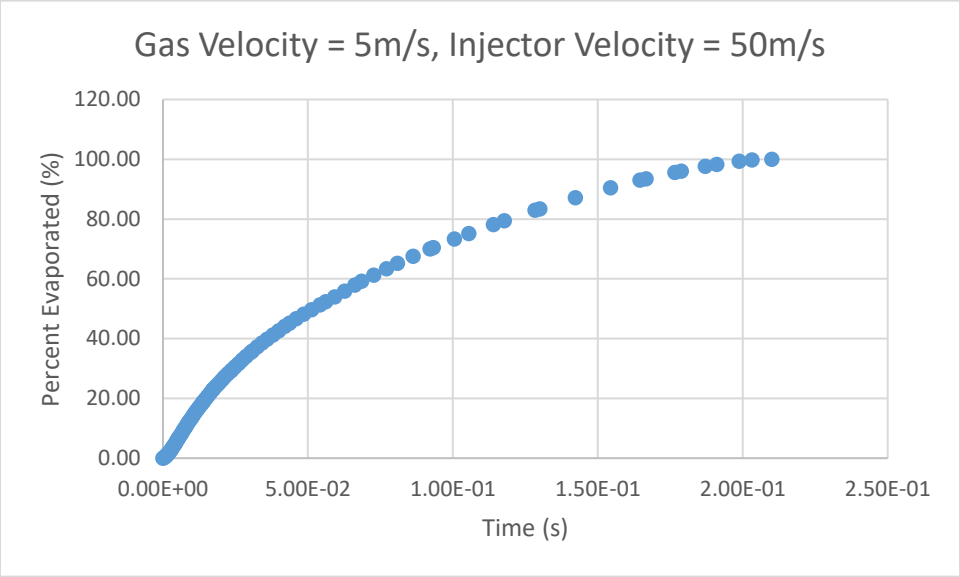

Figure A7 (repeated). Evaporation plot of a water droplet with gas velocity 5 m/s and injection velocity 50 m/s

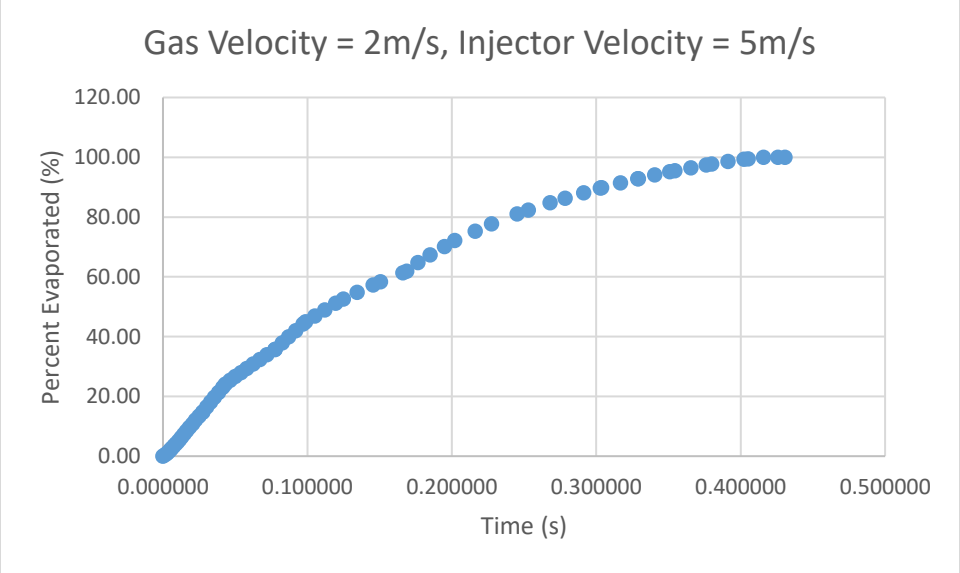

Figure A8. Evaporation plot of a water droplet with gas velocity 2 m/s and injection velocity 5 m/s.

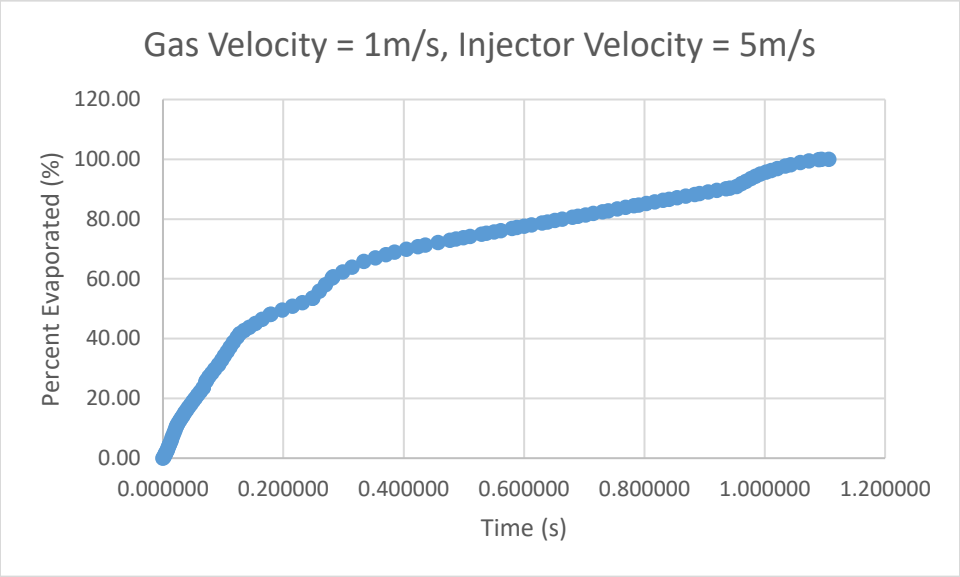

Figure A9. Evaporation plot of a water droplet with gas velocity 1 m/s and injection velocity 5 m/s

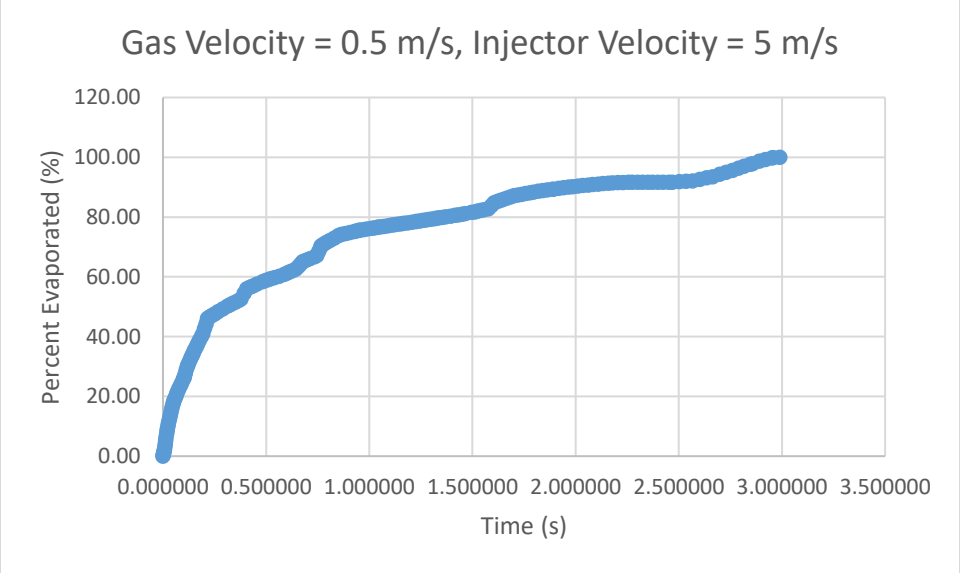

Figure A10. Evaporation plot of a water droplet with gas velocity 0.5 m/s and injection velocity 5 m/s

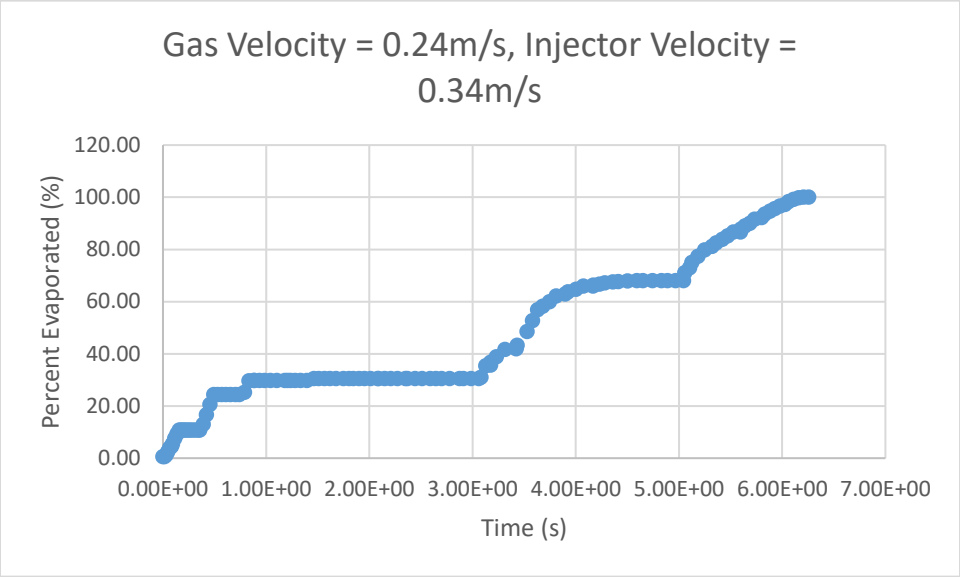

Figure A3 (repeated). Low velocity test of 200 micron drop at 800 C. Evaporation plot of a water droplet with gas velocity 0.24 m/s and injection velocity 0.34 m/s